Effects of Polymerization Media on the Nanoscale Conductivity and Current−Voltage Characteristics of Chemically Synthesized Polyaniline Films

Su-San Chang and Chun-Guey Wu*

Department of Chemistry, National Central University, Chung-Li, Taiwan 32054, Republic of China

Received: June 10, 2005; In Final Form: July 26, 2005

A current sensing atomic force microscope (CS-AFM) was used to probe the conducting homogeneity and band structures of fully doped polyaniline (PANI) films prepared from in situ chemical polymerization/deposition of aniline on indium tin oxide in various inorganic acids. The charge transport properties of PANI films depend on the film thickness as well as polymerization medium. Fluctuations in conductivity are observed on all acid-doped PANI films and the conducting homogeneity was dependent on the film thickness: the conductivity of thick film is more uniform. The current−voltage ($I-V$) characteristics of all thick (>200 nm) films displayed a metal-like behavior and conductivity as high as 40 S/cm was detected in high conducting regions of film thicker than 400 nm. Whereas thin (<120 nm) films revealed insulating, semiconducting, and semimetal conducting, wide distribution in conductivity and interband distances (estimated from the $I-V$ *or* $dI/dV-V$ curves) was found. The interband distances is 0−1.35, 0−1.0, and 0−0.78 eV for thin PANI film prepared from HCl(aq), $HClO_4$(aq), and H_2SO_4(aq), respectively. PANI film (260 nm) prepared from H_2SO_4(aq) revealed fiberlike morphology, and compared to PANI films prepared from HCl(aq) and $HClO_4$(aq) with similar thickness, it has higher average nanoscale conductivity but lower bulk conductivity. This result could be direct evidence which supports that the bulk conductivity of PANI depended on the carriers hopping between the conducting domains.

Introduction

Polyaniline (PANI) is a prominent intrinsically conducting polymer, due to its unique combination of high conductivity, easy preparation, and technological usable products such as films and fibers. It is a phenylene-based polymer having chemically flexible −NH− groups in the polymer main chain flanked on either side by phenylene rings. Many physicochemical properties of PANI are largely dependent upon the extent of −NH− (imine) sites of polymeric backbone and the packing of polymer chains.[1] A lot of research work[2] has been devoted to understanding its structural, thermal, magnetic, and electrical properties, but still many doubts remain.[3] There is also a large amount of scientific work dealing mainly with its charge carriers and the way in which the carriers move in polymer chains and polymer films.[4] It was shown that the localized variations in the thickness, stoichiometry, defects, or even substrates[5] of the PANI films are also factors believed to influence the localized conductivity. Furthermore, among the organic conducting polymers, polyaniline is the only conducting polymer whose properties depend not only on the oxidation state but also on its protonation state/doping level and the nature of dopants. For intermediate protonation levels, magnetic and optical experiments supported the phase segregation between highly conducting regions and the insulating background.[6] The charge conduction was proposed via charging energy-limited tunneling among the small granular polymeric grains.[7] Therefore, Ginder[8] et al. believed that the conductivity of the conducting island in PANI could be up to 10^3 S/cm.

A variety of inorganic[9] and organic dopants[10] have been used with an aim to enhance its stability, conductivity, and processability. Wang[11] et al. found that among the inorganic dopant, sulfuric acid (H_2SO_4) doped PANI has a better stability compared to HCl doped PANI. Elamin[12] et al reported that PANI doped with H_3PO_4 or tartaric acid shows semiconductor behavior and follows a VRH (variable range hopping) mechanism. The conduction mechanism of H_2SO_4 doped PANI studied by Gupta[13] et al. had showed that charge transport is crucially composition dependent. Those studies implied that the dopants have a large impact on the charge transport properties of doped PANI in bulk. Furthermore, it was known[14] that the morphology and conductivity of PANI depended on the synthetic conditions. This is due to the difference in formation mechanism in different polymerization media.[15] It will be interesting to know how the synthetic condition and dopant affects the charge transport properties of PANI films in nanoscale.

Atomic force microscopy with a conducting tip (so-called conducting AMF (C-AFM) or current-sensing atomic force microscopy, CS-AFM) has found its applications in many areas including organic materials.[16] The contact in CS-AFM can be made between the conducting tip and the substrate with a certain confidence by maintaining a prescribed load force. Topographical and current images could be obtained simultaneously for various systems, which provide otherwise impossible information on the conductivity in nanoscale domains. Furthermore, the current−voltage ($I-V$) traces can provide the relations between structural features and electrical properties of the materials on the nanometer scale.[17] Recently, we had reported[18] the spatial variations in electric conductivity and band structures of polyaniline films prepared from in situ polymerization/deposition of aniline on indium tin oxide (ITO) substrates[19] in HCl(aq) using CS-AFM. In the present report, a CS-AFM technique is used to image the heterogeneous electronic conductivity of PANI films prepared from various solutions of

* Corresponding author. E-mail: t610002@cc.ncu.edu.tw. Tel: 011886-3-422-7151 ext 65903. Fax: 011886-3-422-7664.

10.1021/jp0531210 CCC: $30.25
Published on Web 09/13/2005

TABLE 1: λ_{max} of PANI Films Prepared from Various Acidic Solutions

HCl(aq)[a]			$HClO_4$(aq)			H_2SO_4(aq)		
thickness (Å)	λ_{max} of EB (nm)	λ_{max} of ES (nm)	thickness (Å)	λ_{max} of EB (nm)	λ_{max} of ES (nm)	thickness (Å)	λ_{max} of EB (nm)	λ_{max} of ES (nm)
111	545−592	884	111	541	994	116	578	767
183	590	888	224	578	1080	193	584	780
276	576	928	297	625	1236	261	592	775
395	604	912	350	624	1263	346	592	786
477	597	887	440	625	1261	471	589	784

[a] Some data were taken from a previous report.[18]

inorganic acids and doped with diverse dopants. The morphology related charge transport phenomenon is emphasized.

Experimental Section

Chemicals. Water was purified using a Milli-Q (Millipore Corp., Bedford, MA) purification system with a resistivity of 18 MΩ cm. ITO substrate (Merck Display Technologies Ltd. with ITO thickness of 100 nm and surface resistance of ∼20 Ω/□) was cut into 20 × 20 mm. Aniline (ACROS-BACS grade) was used after distillation over calcium hydride powder and stored in the dark under a nitrogen atmosphere. HCl(aq), $HClO_4$(aq), H_2SO_4(aq), NH_4OH(aq), and $(NH_4)_2S_2O_8$ were obtained from commercial resources and used without further treatment.

Preparation of PANI Films and Polymer Molecular Weight Determination. Polyaniline films on ITO substrates were prepared as reported in the literature.[19] $HClO_4$(aq) and H_2SO_4(aq) as well as HCl(aq) (concentration 1.2 M) were used in the polymerization processes. Prior to analysis, each sample was first dipped in 0.1 M NH_4OH(aq) (to ensure that it is fully dedoped to emeraldine base (EB)) for 2 min, washed with distilled water, and dried under a stream of N_2 gas. The film thickness was determined by a Veeco Instruments Dektak3 surface profiler, scanning electron microscopy (SEM) micrographs, and the absorption intensity at 600 nm. The doping (protonation) process was carried out by dipping the EB films into the 0.1 M acidic solution, and the UV−vis spectra were used to monitor the doping levels of PANI films. Upon being dipped in acid, EB converts to emeraldine salt (ES), and the λ_{max} shifts to higher wavelength. The PANI films are fully doped/protonated when λ_{max} of ES stopped increasing. The weight-average molecular weights of the polymers were determined by gel permeation chromatography (GPC) on a Waters-2487 instrument using NMP as an eluent and polystyrene as standards.

CS-AFM Studies. Samples for CS-AFM studies were mounted, via silver paste, to the AFM sample holder. The contact mode AFM with a current-sensing module (SPA400, SEIKO Inc., Japan) was used to simultaneously obtain topographical and current images. The detailed experimental procedures and data analysis were reported previously.[18]

Charge Transport Measurements. The bulk conductivity of PANI was measured using the constant-current, four-probe method on pressed pellet of PANI powder and PANI film. Silver paste was applied to make the electrical contacts. A Keithley 238 programmable electrometer was used to provide a constant current from the two outer probes and to measure the voltage drop between the two inner probes. The floating potential across two inner electrodes was measured to determine the conductivity.[20]

Results and Discussion

Synthesis of PANI Films in Various Inorganic Acids or Doped with the Same Acids As Used in the Polymerization Procedure. PANI films used in this study were prepared by in situ polymerization/deposition of aniline on ITO in acidic aqueous solutions at 0 °C. The thickness (100−500 nm) of PANI films was controlled by the deposition time. In general, it takes longer to deposit PANI films with similar thickness (110 nm) when the polymerization reaction was carried out in $HClO_4$ and H_2SO_4 media (50 and 30 min, respectively) compared to that carried out in HCl(aq) (20 min). To measure the thickness (using UV−vis spectrum) and exchange dopants, the as-prepared films were dipped in 0.1 M NH_4OH(aq) for 2 min to convert ES to undoped EB. Doping of PANI films was carried out by dipping the EB film in 0.1 M acidic aqueous solution. To fully dope the PANI films, $HClO_4$(aq) and H_2SO_4(aq) take much longer (ca. 300 s) compared to HCl(aq) (ca. 20−60 s). The rate of protonation depended on the type of dopant but not on the origin of EB. In other words, it takes similar time to fully dope EB prepared from HCl(aq), $HClO_4$(aq), and H_2SO_4(aq) with HCl. The λ_{max} of both EB and ES are dependent on the preparation conditions and dopants: The λ_{max} of thick (>200 nm) EB films prepared from $HClO_4$(aq) are longer than those synthesized from HCl(aq) and H_2SO_4(aq). Only ES films prepared from $HClO_4$(aq) and doped with $HClO_4$ have a absorption tail extended to the near-IR range. The absorption maxima for EB and ES films prepared from various acidic solutions in different thickness are summarized in Table 1.

Table 1 revealed that the λ_{max} of both EB and ES films prepared from HCl and H_2SO_4 solutions is independent of film thickness except for very thin EB films grown in HCl(aq). This is due to the fact that it takes a very short time to deposit thin PANI film on ITO in HCl(aq). During this short period of time, the structure of PANI changes rapidly, depending on temperature, environment, oxidant, etc.[21] On the other hand, the λ_{max} of both EB and ES films prepared from $HClO_4$(aq) increased as increasing film thickness up to 300 nm, although the $\pi-\pi$ transition of EB is independent of film thickness. It was known[2b] that longer λ_{max} in EB suggested that the polymer chain has a higher degree of oxidation. $HClO_4$ is an oxidizing acid; PANI may be oxidized further by dipping in $HClO_4$(aq) for a long period of time (vide ante). Does the higher degree of oxidation of PANI chains have any presupposition for the interband energy, conductivity, and conducting homogeneity after doping? The answer is not perceptible. The red-shift in λ_{max} of ES with increasing film thickness was tentatively attributed to the interchain interaction. Furthermore, the λ_{max} of both ES and EB films has some indication on the charge transport of PANI; however, the λ_{max} of ES was determined not only by the λ_{max} of the corresponding EB film but also by film thickness and dopant. These results suggested that the charge transport properties of PANI cannot be derived simply from spectroscopy data.

It is interested to note here that the UV−vis−near-IR spectra of PANI prepared from $HClO_4$ solution and then doped with $HClO_4$(aq) (Figure 1a ∼ 1d) are quite different from spectra of PANI prepared from HCl(aq) and then doped with $HClO_4$

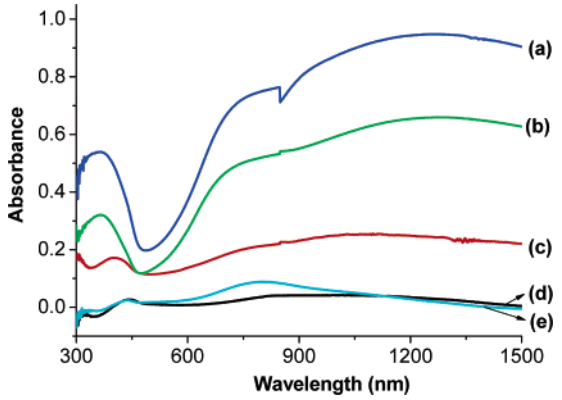

Figure 1. The UV−vis−near-IR spectra of PANI films prepared from (a−d) $HClO_4$(aq), (e) HCl(aq), dedoped with NH_4OH and redoped with $HClO_4$(aq) (the film thicknesses of (a−e) are 440, 348, 224, 111, and 110 nm, respectively).

(Figure 1e). The later has a well-defined peak; nevertheless, the absorption tail extending to the near-IR range (which was assigned to the delocalization of electrons in the polaron band[22] or intraband free carrier excitation[23]) was detected in the former film. This finding indicated that the arrangement and the oxidation state of polymer chains (which depended on the preparation conditions) in EB film affects significantly the electronic structure and therefore the charge transport properties of polymer film after doping.

Local Conductivity and Interband Distances of $HClO_4$ Doped PANI Films Prepared from $HClO_4$ Aqueous Solution. It was shown in the previous paragraphs that the λ_{max} of both EB and ES prepared from $HClO_4$(aq) and doped with $HClO_4$ is not the same as those prepared from HCl(aq) that we reported recently.[18] What are the differences in nanoscale charge transport properties between these two types of PANI films? Figure 2 shows typical topographic (a) and current (b) images obtained simultaneously for an identical part of the surface of $HClO_4$ doped PANI films with various thickness. The globular-shaped structure in the topographical image is observed. This globular-shaped image is a typical topography for PANI films prepared from HCl(aq).[18] The shapes and sizes of the grains observed in the topography images are consistent with the scanning electron microscopy (SEM) images (Figure 3). It was found that PANI films prepared from $HClO_4$(aq) have a smaller grain size and therefore more smooth surface compared to those synthesized from HCl(aq), as revealed with both AFM and SEM images. The current images demonstrate that electron conduction across the PANI film is heterogeneous, regardless the thickness, with localized regions of high (or low) conductivity dispersed within the low (or high) conducting regions. The size of high conducting domains depends on film thickness; thicker film has larger high-conducting domains. Nevertheless, when the PANI film is thicker than 350 nm, the conductivity decreased again, due to the poor continuity and adhesion of the film on ITO substrate. The current for low conducting regions in thin film is very small even at high applied voltage (100 mV). On the other hand, in highly conducting regions of thick films, the current is larger than 100 nA (for the current up limit of the instrument, therefore, we could not distinguish the conductivity between various points on the surface with currents higher than 100 nA) even at very small applied voltage (3 mV, the voltage low limit of the instrument). The distinguished conducting domains were revealed only at certain bias voltages. However, for comparing the conductivity we thus used the same bias voltages (as much as possible) to examine polymer films with various thicknesses, although the distinguished conducting

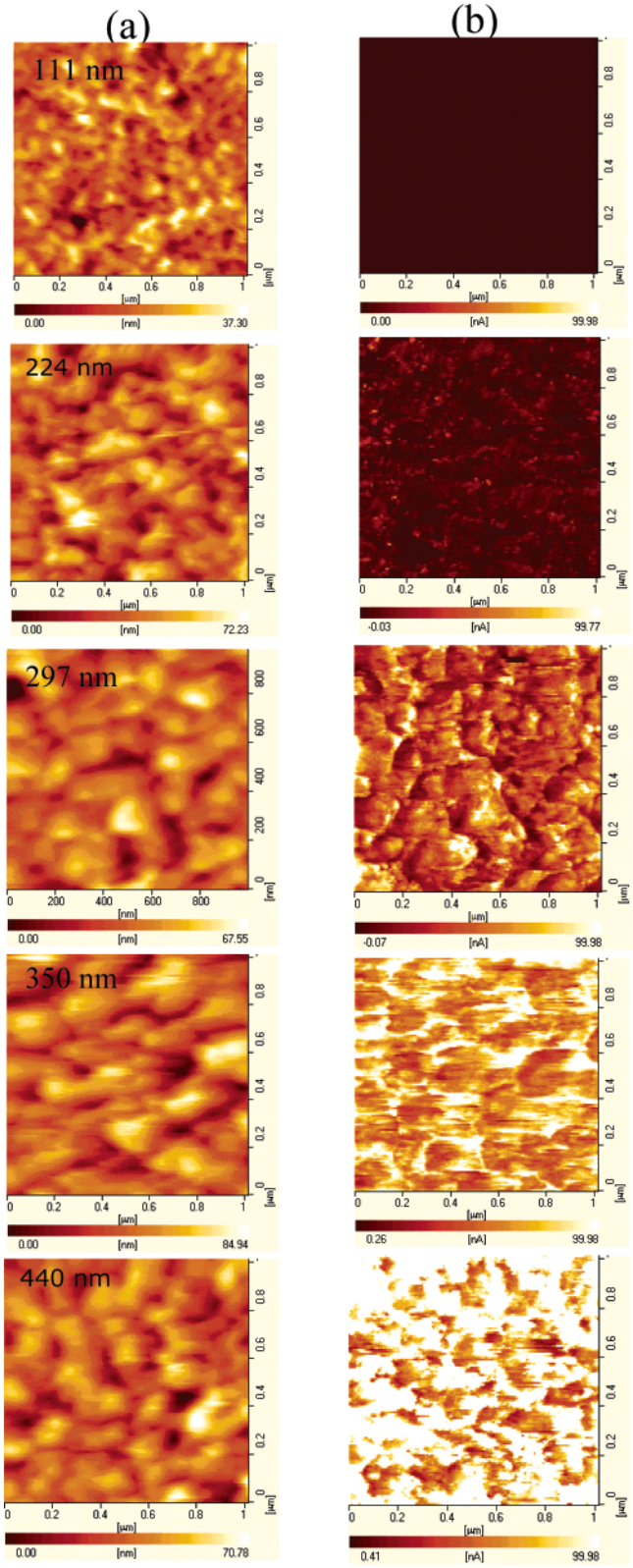

Figure 2. The AFM (a) topographies and (b) CITS images of $HClO_4$ doped PANI films prepared from $HClO_4$(aq). (bias voltage, 0.003 V for 350 nm film and the rest is 0.1 V).

domains may not be revealed clearly. The AFM and current-imaging tunneling spectroscopy (CITS) data of these films are summarized in Table 2.

To follow the evolution of the interband distance[24] of PANI films prepared from $HClO_4$(aq) more quantitatively depending on the thickness, the currents were taken under various bias voltages at three selected spots (the highest conducting area,

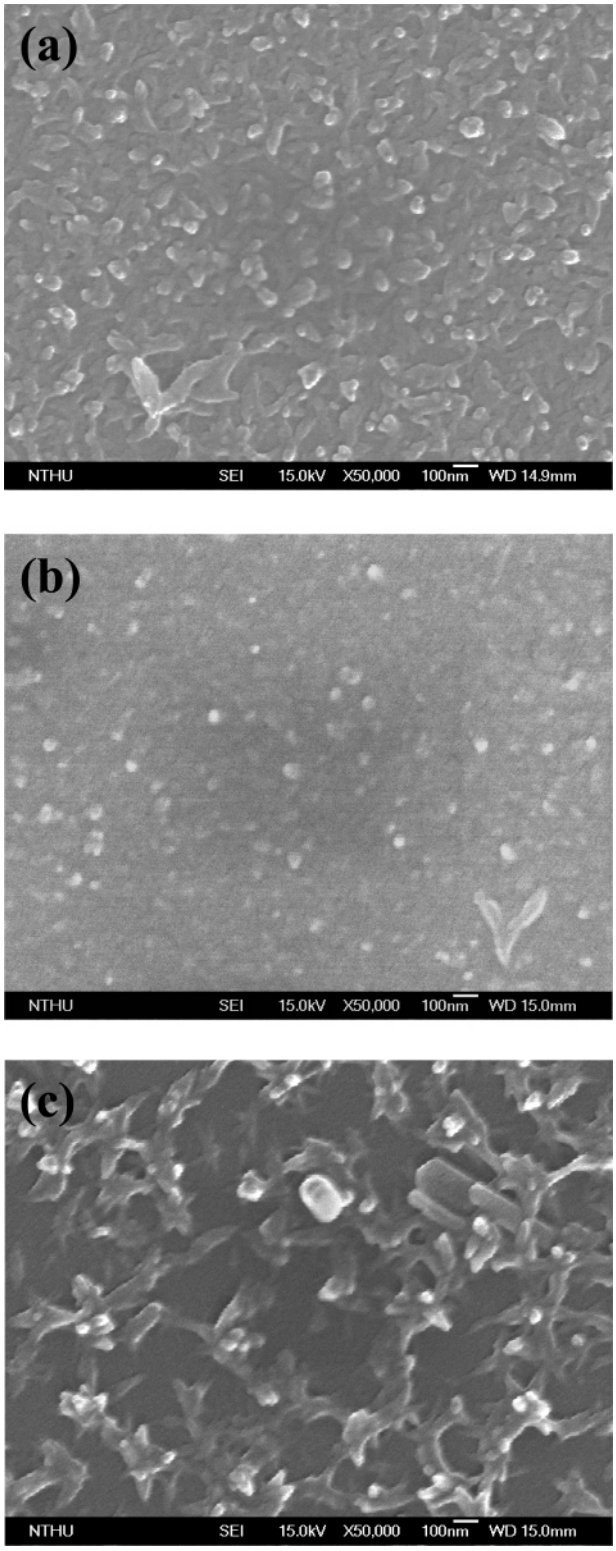

Figure 3. The SEM micrographs of PANI films prepared from (a) HCl(aq), (b) $HClO_4$(aq), and (c) H_2SO_4(aq) and doped with the same acid as used in the polymerization reactions (110 nm film thickness).

the lowest conducting area, and one between them). The electrical characteristics of each region were investigated by recording the tip current (I) as a function of the bias voltage (V). To obtain the $I-V$ curve, I is continuously measured as function of V, which is linearly scanned from +1.6 to −1.6 V at a step of 12.5 mV, the results and the CITS images (the area for measuring the $I-V$ curve may not be the same as that for taking AFM images) of the selected spots are shown in Figure 4. Inspection of the three $I-V$ curves at different spots of thin film (111 nm) reveals that the conductivity of thin film was inhomogeneous and $I-V$ curves with different slopes can be obtained although the current flow at all regions are small (<15 nA at 100 mV for highest conducting area). These curves exhibited semiconductor-like characteristics although the interband distance of low conducting regions is very high (>3.2 eV). The conductivity, σ, within each region in which the current is not limited by the instrument was estimated from the $I-V$ curves using eq 1 and assuming a contact radius between tip and substrate is 50 nm.[24]

TABLE 2: The AFM and CITS Data of PANI Films Prepared from Various Acidic Solutions

polymerization medium	film thickness (Å)	rms (nm)[a]	applied bias (V)	I_{av} (nA)[b]	conducting inhomogeneity[c]
HCl(aq)	111	8.3	0.1	0.24	4.17
	183	12.4	0.01	1.43	1.34
	276	17.6	0.003	2.38	0.83
	395	12.1	0.003	6.94	0.63
	477	19	0.003	>27.2[d]	−[e]
$HClO_4$(aq)	111	5.9	0.1	1.4	0.77
	224	13.9	0.01	2.2	0.67
	297	11.4	0.01	6.23	0.66
	350	14.6	0.003	>87.9	−
	440	13.4	0.003	3.1	0.65
H_2SO_4(aq)	116	13.4	0.1	0.33	1.21
	193	18.8	0.1	5.87	1.13
	261	19.8	0.003	26.1	−
	346	16.0	0.003	>41.1	−
	471	13.0	0.003	>63.3	−

[a] Root mean square of the surface roughness. [b] The average of the current within the measured area (32768 data points in the area of 1 μm × 1 μm). [c] Conducting homogeneity is equal to I_{rms}/I_{av}, where I_{rms} is a root mean square of the current. ($I_{rms} = (\sum(I_i - I_{av})^2/n)^{1/2}$. A smaller value indicates better conducting homogeneity. [d] It means that some points have current higher than 100 nA, the current up limit of the instrument. [e] Cannot be determined, due to some points having current higher than 100 nA.

$$\sigma = d/(\mathrm{A}t R) \qquad (1)$$

σ is the conductivity, and d is the film thickness. At is the area of the C-AFM probe in contact with the surface. At was computed as πr^2, assuming a contact radius between tip and sample is 50 nm. R is the resistance of the sample, estimated from the inverse slope of the $I-V$ curve. When the $I-V$ curve is not linear, the slope of the curve was estimated from the linear fit of the curve.

With this approximation, the conductivities of the all conductive regions in the thin film were estimated to be 1×10^{-2} to 3.0×10^{-6} S/cm, almost 4 orders of magnitude difference in conductivity.

All $I-V$ curves of thick (>220 nm) PANI films displayed metal-like characteristics with the interband distance of 0 eV. Nevertheless, the $I-V$ curves of 220 and 440 nm thick films are not symmetrical with respect to 0 V. This is a behavior generally observed in a typical semiconductor−metal junction: A typical semiconductor−metal junction shows different current responses for forward and reverse biases.[25] Thus, these films can be regarded as a semimetal: a semiconductor with small density of state in the gap, probably due to the introduction of narrow polaron and bipolaron bands within the band gap or the spot contains small metal and insulator domains, which cannot be resolved with an AFM tip. The semiconducting properties derived from doped conjugated polymers could be different from those of true (inorganic) semiconductors. It was known that

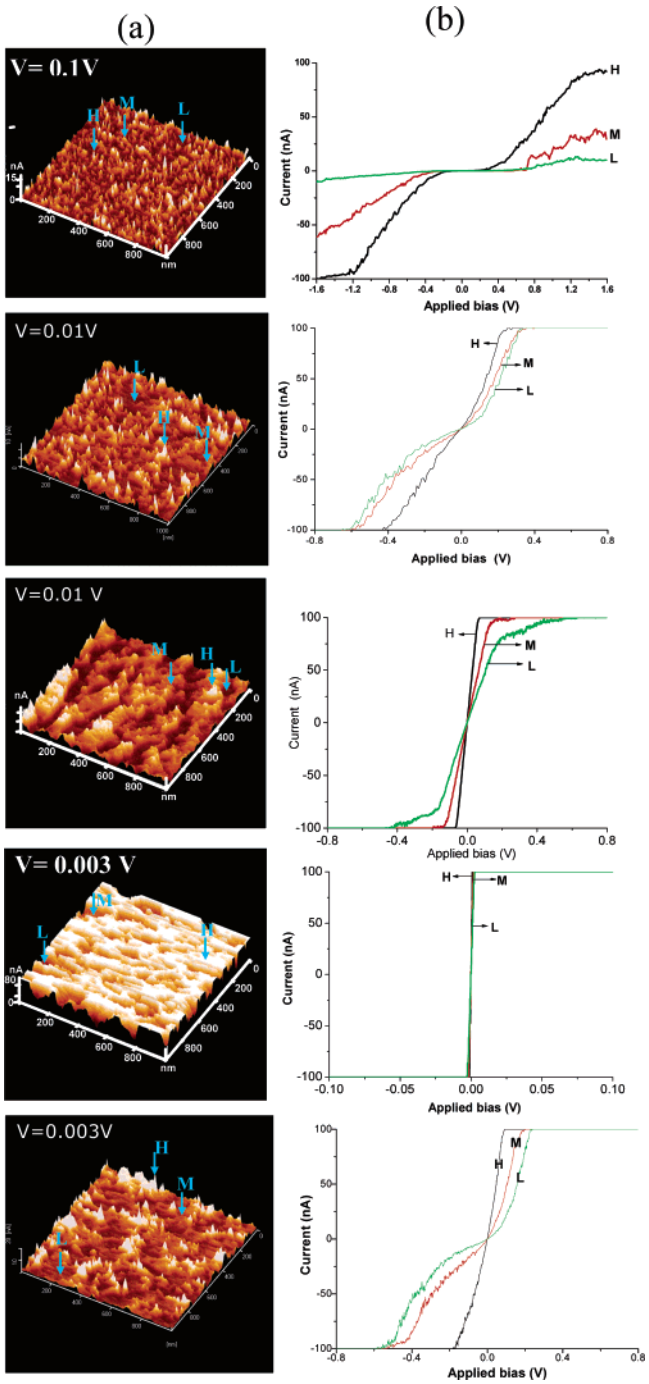

Figure 4. The (a) CITS images and (b) $I-V$ curves of $HClO_4$ doped PANI films prepared from $HClO_4$(aq) (film thicknesses from the top are 111, 224, 297, 348, and 440 nm).

conducting polymers become metal-like conductors when heavily doped[26] because interstate bands arising from bipolarons make the interband distance small enough to make the holes move around rather freely upon applying a bias voltage. Here we found that only heavily doped is not guaranteed for metal-like conducting for PANI films. The truly metal-like conducting behavior revealed when the polymer film (prepared from $HClO_4$-(aq)) was thick enough (>300 nm). These results indicated that the interchain interactions have a large impact on the charge transport properties of fully doped PANI films.

The conductivity data derived from the $I-V$ curves of $HClO_4$ doped PANI films are listed in Table 3. As can be seen in Table 2 and Table 3, thicker PANI films have not only higher conductivity but also better conducting homogeneity. Both

TABLE 3: The Charge Transport Properties of PANI Films Prepared from Various Acidic Solutions

polymerization medium	film thickness (Å)	σ_{max} (S/cm)[a]	$\sigma_{max}/\sigma_{min}$[b]	interband distance (eV)[c]
HCl(aq)	111	0.028	10^5	insulating,[d] 0−1.1, semimetal[e]
	183	0.15	5.35	semimetal
	276	1.05	9.5	metallic
	395	2.78	3.5	metallic
	477	36.0	2.9	metallic
$HClO_4$(aq)	111	0.01	10^3	insulating, 0.3−1.0
	224	0.083	1.7	semimetal
	297	0.59	6.2	metallic
	348	37.9	2.2	metallic
	440	0.42	3.8	semimetal
H_2SO_4(aq)	116	0.003	6.8	0.4−0.85, semimetal
	193	0.13	1.5	semimetal
	261	16.5	11.3	metallic
	346	28.5	5.0	metallic
	471	42.2	2.8	metallic

[a] σ_{max}, the conductivity of the highest conducting regions; σ_{min}, the conductivity of the lowest conducting regions. The data were summarized from several areas of the same film. [b] We measure several areas in each film and Figure 3 and Figure 6 are just some of them. The interband distances are the summary of all measurements, some CITS images and I−V curves did not show in the article. [c] The interband distance was estimated from the I−V curve. The range for the curve with slope close to 0 is defined as the interband distance of the measured point. [d] Insulating represented the band gap of that region is higher than 3.2 eV. [e] Semimetal indicated that in some areas the interband distance is 0 V but the I−V curve showed the semiconducting behavior as described in the text.

insulating and semiconducting regions were detected in $HClO_4$ doped thin film and conductivity differences between highest and lowest conducting regions are up to 3000 times, whereas only metal-like conducting was found in thick films and the conductivity difference is less than 6 times. It is worth noting here that thick (>350 nm) films prepared from $HClO_4$(aq) are not as stable as those synthesized from HCl(aq)[18] and H_2SO_4-(aq) (vide infra). The poor adhesion and continuity made $HClO_4$ doped thick film less conducting and acted like a semimetal. Another special feature in PANI films prepared from $HClO_4$-(aq) is the abrupt increasing in conductivity from 300 to 350 nm. This phenomenon may relate to the film deposition mechanism. The nucleation and growth mechanism of polyaniline had been studied with transient electrochemical techniques.[15] A "three-dimensional instantaneous nucleation under charge-transfer control" was proposed[15a] for electrochemical deposition of PANI film in $HClO_4$(aq). If the similar mechanism was applied to the chemically deposited PANI films, we may expect at certain film thickness (such as 224 nm) that small (smaller than the contact radius between tip and sample) and discontinuous conducting islands will form. This film will have a low conductivity and is expected to show a semimetal conducting behavior. These small conducting islands continues to grow as film gets thicker and finally contact with each other to form large conducting domains; therefore, metal-like conducting is revealed. A paper reported by Park[27] et al. recently showed that PANI film (1 μm thickness) electrochemically grown from $HClO_4$(aq) has very low conductivity (4.6×10^{-3} S/cm). This value is much lower than those that we have obtained for PANI thin film chemically grown in $HClO_4$(aq). All these data indicated that thick PANI films prepared in $HClO_4$(aq) have a poor quality even though the film thickness, the substrate, the parameters for the CS-AFM studies and the equation for calculating the conductivity used by Park are different from what we have used.

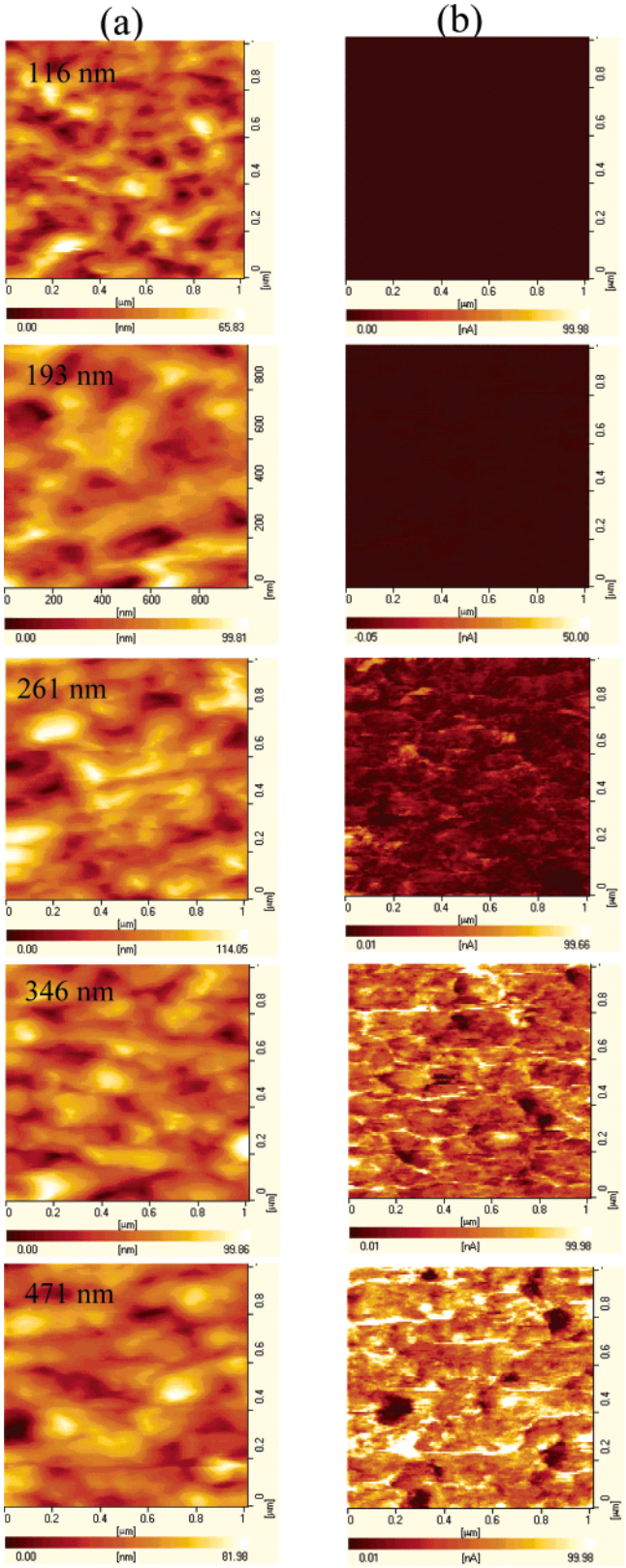

Figure 5. The AFM (a) topographies and (b) CITS images of H_2SO_4 doped PANI films prepared from H_2SO_4(aq) (0.003 V bias voltage).

Local Conductivity and Interband Distances of H_2SO_4 Doped PANI Films Prepared from H_2SO_4 Aqueous Solution. The topography and CITS images of H_2SO_4 doped PANI films prepared from H_2SO_4(aq) in various thicknesses are shown in Figure 5 and the data are also listed in Table 2. The globular-like structure is also observed in thick PANI films. Nevertheless, fibril morphology (which was noted in electrochemical prepared PANI film using H_2SO_4(aq) as an electrolyte[28]), see Figure 3, was detected in thin film. The conducting inhomogeneity was also observed in all H_2SO_4 doped PANI films regardless of the film morphology and thickness. In general, thicker film has a higher conductivity and better conducting homogeneity as also observed in PANI films prepared from HCl(aq)[18] and $HClO_4$-(aq). Surprisingly, thick (>200 nm) PANI films prepared from H_2SO_4(aq) has a higher average nanoscale conductivity than those prepared from HCl(aq).[18] Comparing these current image data with the optical data shown in Table 1, we found that the degree of oxidation of polymer chains prepared from H_2SO_4-(aq) and HCl(aq) is similar (their EB forms have a similar λ_{max}) and the λ_{max} of ES (the band is assigned to the transition from the π to polaron band or interband excitation according to Xie[29] et al.) synthesized from H_2SO_4 solution is shorter than that synthesized from HCl(aq). In other words, PANI films synthesized from H_2SO_4 solution need more energy for the interband excitation; therefore may be expected to have a lower conductivity, contradictory to what we have observed. These results suggested that the conductivity of PANI films in nanoscale cannot be predicted only by their electronic spectra. The UV−vis−near-IR spectra of PANI thick film prepared from H_2SO_4-(aq) were also not the same as those synthesized from $HClO_4$(aq). The H_2SO_4 doped film has a localized polaron band, and free carrier tail was observed in $HClO_4$ doped film. However, it is hard to compare the dopant related conducting behaviors between H_2SO_4 and $HClO_4$ doped PANI films at various thicknesses, since $HClO_4$ doped PANI films act irregularly (vide ante).

As disclosed in the previous paragraphs and previous study,[18] the morphology, conductivity, conducting homogeneity, and $I-V$ characteristics of the HCl and $HClO_4$ doped PANI films are dependent on the film thickness. In efforts to explore the effects of film thickness on the charge transport properties of PANI prepared from H_2SO_4(aq), we measured the $I-V$ curves of several films at some selected spots and the results are shown in Figure 6. As can be seen, the $I-V$ curves in various conducting regions of thick (>240 nm) films displayed metal-like characteristics. The $I-V$ curve revealed an ohmic response and the current saturated at the bias voltage as small as 0.05 V. Furthermore, all $I-V$ curves are rather symmetrical with respect to 0 V, a typical behavior of a resistor. The conductivity of the highest conducting region of thick (477 nm) film calculated from eq 1 is 42 S cm^{-1}, which is 2.8 times that for a low conducting region at the same film. This result indicated that thick film prepared from H_2SO_4(aq) has good conductivity and conducting homogeneity. Nevertheless, the $I-V$ curves of thin (116 nm) film revealed only semiconducting regions with various interband distances and conductivities. The interband distances evaluated from the differential conductance were in the range of 0−0.78 eV. The conductivity as low as 3.8×10^{-4} S/cm was found in the low conducting region. When the thickness of film increased to 260 nm, no semiconducting regions were detected; only metal-like conducting was observed. The $I-V$ curves of all conducting regions have an ohmic response, and the $I-V$ curves are all symmetrical with respect to 0 V. These results also supported that the electric properties of PANI films were affected by the aggregation and arrangement of the polymer chains. To ensure the metallic conducting behavior, a sufficient amount of polyaniline chains with few structure defects must be amassed in a polymer film. In PANI films prepared from H_2SO_4(aq) we also observed an abrupt increase (>100 times) in conductivity from 200 to 260 nm. It can be

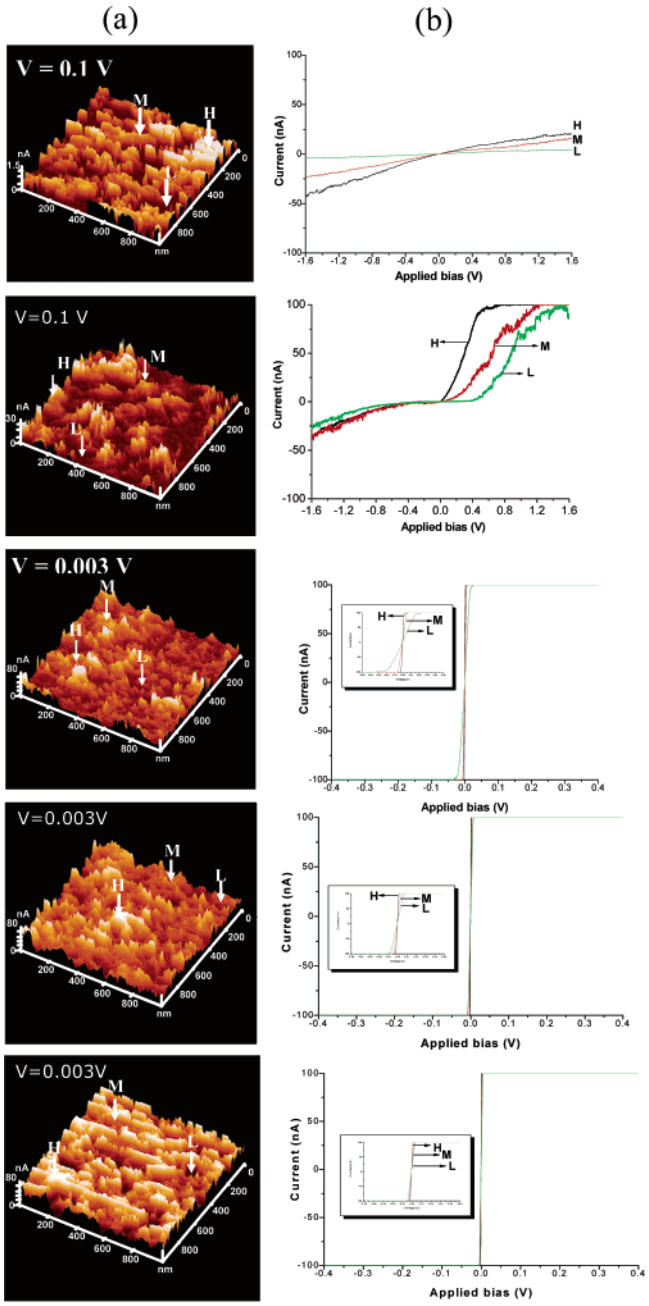

Figure 6. (a) CITS images and (b) $I-V$ curves of H_2SO_4 doped PANI films prepared from H_2SO_4(aq). (film thicknesses from the top are 116, 193, 261, 346, and 471 nm).

attributed to the size of PANI fiber large enough to show the metal-like conductivity in this thickness.

The Effects of Polymerization Medium on the Charge Transport Properties and Conducting Homogeneity of Chemical Polymerized, Inorganic Acid Doped PANI Films. A large fluctuation in film conductivity was observed in fully doped PANI film prepared from both $HClO_4$(aq) and H_2SO_4-(aq) as well as HCl(aq),[18] although the morphologies are different among them. For example, the height-mode image of the region of interest shows that thin (~110 nm) PANI film prepared from H_2SO_4 solution has a fibril-like structure (Figure 3c and Figure 5a), whereas globular-shaped topography was revealed in thin films synthesized from $HClO_4$ and HCl aqueous solutions, but the former has a smoother surface. The corresponding current image of the similar morphology, however, reveals a different conductivity: the average conductivity of thin PANI films prepared from $HClO_4$(aq) is better than that prepared from HCl(aq) and H_2SO_4(aq). This trend is consistent with the chain length of PANI. The weight average molecular weight of PANI grown in HCl(aq), $HClO_4$(aq), and H_2SO_4(aq) is 19000, 31000, and 28000, respectively. On the other hand, the morphologies of thick (>250 nm) PANI films prepared from HCl(aq), $HClO_4$(aq), and H_2SO_4(aq) are similar, the conductivity of highest conducting region are not the same and the nanoscale average conductivity of PANI obtained from H_2SO_4(aq) is the highest. These results reveal that the conductivity of PANI films is not determined simply by the polymer chain length, even in the nanoscale. Furthermore, the nanoscale conductivity is not directly related to the electronic spectra as described previously. These very complicated relationships between structure, morphology, dopant, thickness, chain length, chain aggregation/arrangement, and conductivity may account for a large difference in opinion in the charge transport mechanism of polyaniline reported in the literature.

It is seen fairly clearly from the current image shown in Figures 2b and 5b that the conducting homogeneity of all thin PANI films is very poor. For example, the conductivity of highest conducting domain is 10^5, 10^3, and 6.8 times higher than the lowest conducting region for films prepared from HCl-(aq), $HClO_4$(aq), and H_2SO_4(aq), respectively. The conducting inhomogeneity is perhaps due to the fact that PANI chains in some regions are more ordered and, thus, more conductive than other regions. The CITS data cannot provide directly the assessment of the difference in chemical identity between high and low conductive regions. However, the high conducting regions likely correspond to better ordered PANI chains previously identified by spectroscopic methods.[30] It seems that both film deposition process (reaction media) and dopant affect the conducting behaviors of the resulting films. However, we have no answer for which one is the predominant parameter at this moment. More experiments are underway to solve this puzzle and the results will be reported later. It is worth noting here that regardless the polymerization medium and dopants, true metal-like conducting was detected only in films thicker than 200 nm. This general phenomenon strongly suggested that without stretching, a sufficient amount of PANI chains must be assembled together to ensure the metallic behavior. This result provides a thought for people who want to use conducting polyaniline nanowires in nanoscale electronic devices. Another interesting observation in this study is that the average nanoscale conductivity of PANI film synthesized from H_2SO_4(aq) is higher but the bulk conductivity is lower than that prepared from HCl-(aq) (0.23 vs 0.37 S/cm). This result could be evidence showing that the bulk conductivity of PANI mainly depended on the carriers hopping between the conducting domains.

Conclusions

Ex situ CS-AFM is an excellent tool for measuring the local conductivity and current−voltage ($I-V$) characteristics of conducting polymers. It was used successfully to visualize the heterogeneous electric properties of chemically prepared conducting PANI films on ITO substrates. The doped PANI thin films, in all dopants and preparation conditions studied in this article, displayed an inhomogeneous conductivity. Current images of fully doped PANI thin (110 nm) films recorded in air demonstrate that the electric conductivity of the highest conducting regions is 10^5 times higher than that of the lowest conducting regions. The large spatial variations in the film conductivity on topographically featureless regions were tentatively attributed to the presence of nanoscale crystallites of polaron lattice. Polymerization conditions influence not only

the morphology but also the charge transport and conducting homogeneity of doped PANI films. Nevertheless, regardless of the preparation medium and dopant, metal-like conducting behavior was revealed only in PANI film thicker than 200 nm. The relationship between the film morphology/thickness and charge transport properties in nanoscale gives more evidence for supporting the charge hopping conduction mechanism.

Acknowledgment. Financial assistance for this research was provided by the National Science Council, Republic of China (Grant Number NSC 93-2113-M-008-005).

References and Notes

(1) dos Santos, M. C.; Bredas, J. L. *Phys. Rev. B* **1989**, *40*, 1997.

(2) (a) Krinichnyl, V. I.; Chemerisor, S. D.; Lebedev, Y. S. *Phys. Rev. B* **1997**, *55*, 16233. (b) Trivedi, D. C. In *Handbook of Organic Conductive Molecules and Polymers*; Nalwa, H. S., Ed.; Wiley: New York, 1997; Vol. 3, Chapters 11 and 14.

(3) Van, M.; Yang, J. J. *J. Appl. Polym. Sci.* **1995**, *55*, 399.

(4) (a) Pouget, J. P.; Jozefowica, M. E.; Epstein, A. J.; Tang, X.; MacDiarmid, A. G. *Macromolecyles* **1991**, *24*, 779. (b) Epstein, A. J.; Ginder, J. M. *Synth. Met.* **1987**, *18*, 303. (c) MacDiarmid, A. G.; Epstein, A. J. *Synth. Met.* **1989**, *29*, E409. (d) Lux, F.; Hinrichsen, G.; Krinichnyi, V. I.; Nazarova, I. B.; Cheremisow, S. D.; Pohl, M. M. *Synth. Met.* **1993**, *55*−*57*, 347. (e) Epstein, A. J.; MacDiarmid, A. G.; Pouget, J. P. *Phys. Rev. Lett.* **1990**, *65*, 664. (f) Ginder, J. M.; Richer, A. F.; MacDiarmid, A. G.; Epstein, A. J. *Solid State Commun.* **1987**, 61, 97. (g) Epstein, A. J.; Ginder, J. M.; Zuo, R. W.; Bigelow, H. S.; Woo, D. B.; Tanner, A. F.; Richer, A. F.; Huang, W.; MacDiarmid, A. G. *Synth. Met.* **1987**, *18*, 303.

(5) (a) Basame, S. B.; White, H. S. *J. Phys. Chem.* **1995**, *99*, 16430. (b) Basame, S. B.; White, H. S. *J. Phys. Chem. B* **1998**, *102*, 9812. (c) Boxley, C. J.; White, H. S.; Gardner, C. E.; Macpherson, J. V. *J. Phys. Chem. B* **2003**, *107*, 9677.

(6) Choi, H. Y.; Mele, E. J. *Phys. Rev. Lett.* **1987**, *59*, 2188.

(7) Abeles, B.; Sheng, P.; Coutts, M. D.; Arie, Y. *Adv. Phys.* **1975**, *24*, 407.

(8) Ginder, J. M.; Epstein, A. J.; MacDiarmid, A. G. *Synth. Met.* **1989**, *29*, E395.

(9) (a) Zuo, F.; Angelopoulus, M.; MacDiarmid, A. G.; Epstein, A. J. *Phys. Rev. B.* **1989**, *39*, 3570. (b) Singh, R.; Arora, V.; Tandon, R. P.; Chandra, S.; Kumar, N.; Mansingh, A. *Polymer* **1997**, *38*, 4897.

(10) Reghu, M.; Cao, Y.; Moses, D.; Heeger, A. J. *Phys. Rev. B.* **1993**, *47*, 1758.

(11) Wang, Y.; Rubner, M. F. *Synth. Met.* **1992**, *47*, 255.

(12) Elamin, A. M.; Liu, Z. L.; Yao, K. I. *Acta Phys. Sin.-Overseas ed.* **1997**, *7*, 458.

(13) Luthra, V.; Singh, R.; Gupta, S. K.; Mansingh, A. *Curr. Appl. Phys.* **2003**, *3*, 219.

(14) Zhang, Z.; Wei, Z.; Wan, M. M*acromolecules* **2002**, *35*, 5937.

(15) (a) Cordova, R.; Valle, M. A.; Arratia, A.; Gomez, H.; Schrebler, R. *J. Electroanal. Chem.* **1994**, *377*, 75. (b) Choi, S. J.; Park, S. M. *J. Electrochem. Soc.* **2002**, *149*, E26.

(16) (a) Kelley, T. W.; Granstrom, E. L.; Frisbie, C. D. *Adv. Mater.* **1999**, *11*, 261. (b) Gardner, C. E.; Macpherson, J. V. *Anal. Chem.* **2002**, *74*, 576A.

(17) (a) Liau, Y.-H.; Scherer, N. F.; Rhodes, K. *J. Phys. Chem. B* **2001**, *105*, 3282. (b) Planes, J.; Houze, F.; Chretien, P.; Schneegans, O. *Appl. Phys. Lett.* **2001**, *79*, 2993. (c) Gadenne, M.; Schneegans, O.; Houze, F.; Chretien, P.; Desmarest, C.; Sztern, J. Gadenne, P. *Physica B* **2000**, *279*, 94. (d) Macpherson, J. V.; De Mussy, J. P. G.; Delplancke, J. L. *J. Electrochem. Soc.* **2002**, *149*, B306.

(18) Wu, C.-G.; Chang, S. S. *J. Phys Chem. B.* **2005**, *109*, 825.

(19) Wu, C.-G.; Hsiao, H.-T.; Yen, Y. R. *J. Mater. Chem.* **2001**, *11*, 2287.

(20) Smiths, F. M. *Bell Syst. Tech. J.* **1958**, 710−718.

(21) Chiou, Y. H.; Wu, C.-G. *J. Chin. Chem. Soc.* **1997**, *44*, 511.

(22) MacDiarmud, A. G.; Epstein, A. J. *Synth. Met.* **1994**, *65*, 103.

(23) Cao, Y.; Smith, P. Heeger, A. J. *Synth. Met.* **1989**, *32*, 263.

(24) Ouyang, M.; Huang, J.-L.; Lieber, C. M. *Annu. Rev. Phys. Chem.* **2002**, *53*, 201.

(25) Park, W. I.; Yi, G.-C.; Kim, J.-W.; Park, S.-M. *Appl. Phys. Lett.* **2003**, *82*, 4358.

(26) Park, S. M. *J. Electrochem. Soc.* **2002**, *149*, E26.

(27) Han, D.-H.; Park, S.-M. *J. Phys. Chem. B* **2004**, *108*, 13921.

(28) (a) Sariciftci, N. S.; Heeger, A. J.; Cao, Y. *Phys. Rev. B* **1994**, *49*, 5988. (b) Stafstrom, S.; Bredas, J. L.; MacDiarmid, A. G. *Phys. Rev. Lett.* **1987**, *59*, 1464.

(29) Xie, Y.; Wiesinger, J. M.; MacDiarmud, A. G.; Epstein, A. J. *Chem. Mater.* **1995**, *7*, 4430.

(30) (a) Krohnke, C.; Enkelmann, V.; Wegener, G. *Angew. Chem.* **1980**, *92*, 941. (b) Pelster, R.; Nimtz, G.; Wessling, B. *Phys. Rev. B* **1994**, *49*, 12718. (c) Lux, F.; Hinrichsen, G.; Krinichnyi, V. I.; Nazarova, I. B.; Cheremisow, S. D.; Pohl, M. M. *Synth. Met.* **1993**, *55*−*57*, 347.